Integrated Physics Lab Report: Thin film and characterization

BHAVANI PRASAD BEHERA

Roll - 2011044
Int. M.Sc - 4th year
School of Physical Sciences

November 26, 2023

Abstract

Thin film techniques have gained significant importance in the development of electronics and nanoscale technologies. In this experiment, we study two physical vapor deposition techniques - resistive thermal deposition system and electron beam thermal deposition system. The latter is used for making nickel-thin films, which are then characterized using XRR and XRD measurements. The thickness of the thin film was found to be 729.22 Å, whereas the roughness was found to be 12.47 Å. The nickel-thin film was then used to measure the sheet resistance of nickel, and finally, the resistivity of nickel was calculated. The resistivity was found to be $(2.452 \pm 0.0044) \times 10^{-7} \Omega m$.

Introduction

Thin film technology can be regarded as one of the major keys in creating electronic devices such as computers since those devices incorporate structures made from thin film deposition. The first thin film deposition was done via electroplating. However, vacuum technology, which is crucial for modern deposition systems, was not developed until 1852. The sputter deposition is the first efficient and well-controlled thin film coating developed.

Thin film deposition systems can be broadly classified into four categories,

- Evaporative methods - Here, the source is heated to form vapors, which are then condensed on the substrate to form thin films.
- Glow discharge processes - These include sputtering techniques, where the surface atoms are ejected from the electrode by bombarding the surface with ions, thus creating a vapor of the electrode material, which is deposited on the target.
- Gas-phase chemical processes - Methods of film formation by purely chemical processes in the gas or vapor phases include chemical vapor deposition and thermal oxidation. Chemical vapor deposition (CVD) is a materials synthesis process whereby constituents of the vapor phase react chemically near or on a substrate surface to form a solid product. In thermal oxidation, the substrate itself provides the source of the metal or semiconductor constituent of the oxide. Hence, it is limited as compared to CVD.
- Liquid phase chemical processes - These include mechanical techniques such as liquid phase epitaxy, spray pyrolysis and electro-processes such as electroplating and electrolytic anodization.

The quality of thin films is judged by characterizing them, which usually includes measuring their thickness, roughness, composition, and purity. Various techniques are used for thin film characterization, like X-ray diffraction, Scanning electron microscopy, transmission electron microscopy, and UV-vis spectroscopy. Thin film properties do not always resemble those at bulk levels, allowing for novel applications.

In this experiment, we have used an electron beam physical vapor deposition system to deposit nickel thin films on silicon substrates. The initial objective was to use a thermal evaporation system to get nickel film deposits on a glass substrate. However, the machine had some issues while creating a vacuum to the desired levels. We attempted to fix it but switched to an electron beam vapor deposition system. This report contains a background of the thin film deposition systems we have come across and the vacuum systems that were used in these machines, the characterization techniques employed in this experiment and their analysis, and the objectives for the next part of this experiment.

Thin film deposition systems

Thermal evaporation system

Thermal evaporation deposition is a common method of physical vapor deposition (PVD) used to deposit thin films. In this process, a solid material is heated inside a high vacuum chamber until vapor pressure is produced. The evaporated material, or vapor stream, then coats the substrate to form a thin film. The process can be performed using a resistive heat source or an electron beam, and the deposition rate can be controlled using quartz crystal rate sensors, temperature, or optical monitoring systems. The thermal evaporation process can be used to deposit both metals and nonmetals, including aluminum, chrome, gold, indium, and many others. The process is commonly used to create metal bonding layers in devices such as OLEDs, solar cells, and thin-film transistors. The advantages of thermal evaporation deposition include simplicity of operation, proper speed, high deposition rate, and material utilization efficiency. The process is widely used in various industries, including optics, electronics, and solar cells.

The thermal evaporation system used in this experiment is a vacuum box coater. Fig 1-4 shows the sections of the machines.

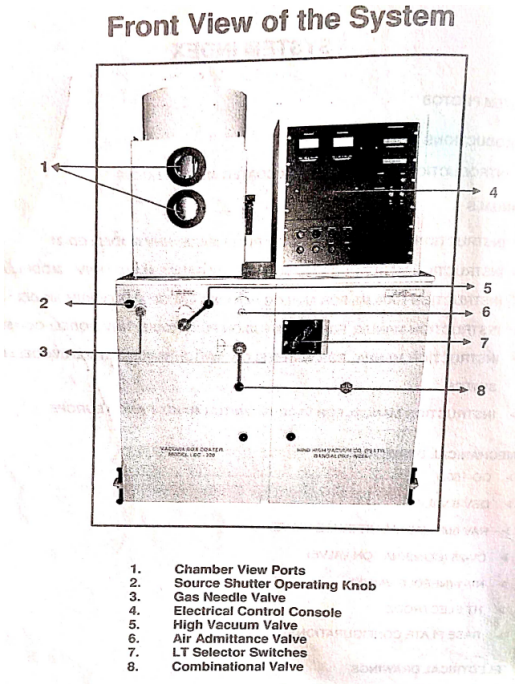

Figure 1: Front view of the box coater

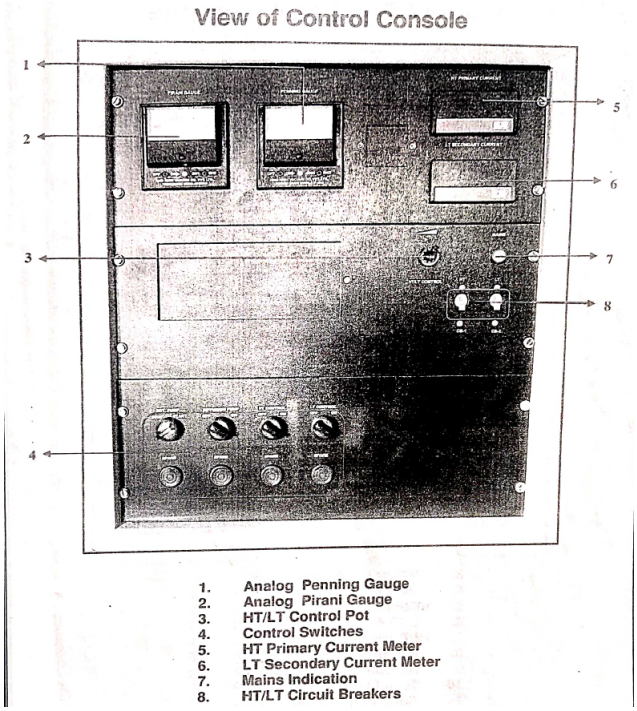

Figure 2: Control console of the box coater

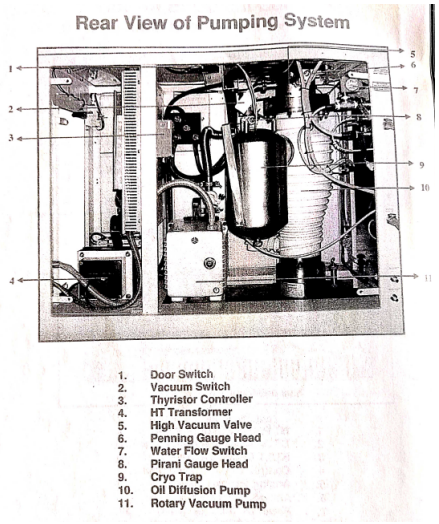

Figure 3: Pumping system of the box coater

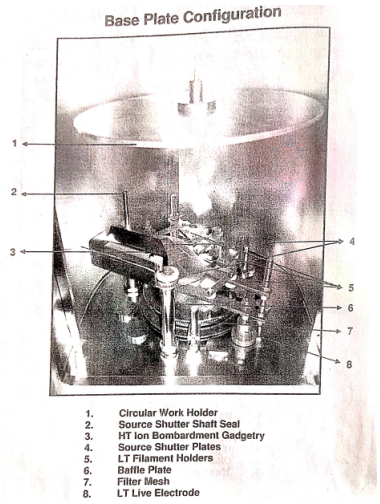

Figure 4: Interior section of vacuum chamber

The vacuum chamber

The vacuum chamber is the area where the deposition of the thin films takes place. Figure 4 shows the interior of the chamber. It consists of a work holder for attaching the substrates, and LT filament holders for holding the baskets or boats with the metal source inside. These are connected to the LT live electrodes to supply the filament's current. Source shutter plates cover the work holder from the metal source. This shutter is manually operated from outside using a switch. Two sets of off-sector filament holders and one set of center filament holders are supplied, each with a set of LT electrodes for multi-layer coatings on small plane areas. A 200 amps selector switch is provided on the door to select any one of the three electrodes. A baffle plate is provided within the tripod above the base plate aperture. This acts as a radiation shield when the radiant heater is used. A stainless steel wire mesh is provided over the base plate opening to prevent foreign bodies from falling into the baffle valve.

The vacuum pump

The section responsible for creating and measuring the vacuum consists of the rotary vane pump, the oil diffusion pump and the gauges (Penning and Pirani gauge).

Rotary vacuum pumps

This is a double-staged, oil-sealed, direct driven, vane type vacuum pump. Both the first and the second stage are isolated with the introduction of an isolator in between and the two rotors are mounted eccentrically within the respective stators. The first stage end plate has a bearing and an oil seal for isolation from the atmosphere. The second stage end cover also has a bearing for locating the shaft. An oil pump housing is mounted on the rear end plate of the stator. It provides the lubrication to the pump and the oil flow to the stator. The pump has a vane which drives the oil under the pressure. A filter is provided on the oil pump housing through which oil is sucked in. Thsi prevents any dirt or other particles from entering the pump and causing reduction in the oil flow and hence causing seizure of moving parts.

During operation, the rotor vanes sweep the volume of the gas or the air trapped in the crescent shaped gap formed by the rotor which is mounted eccentrically in the stator. As each vane passes, the inlet port opening lets in a known quantity of gas which is subsequently trapped and compressed by the next vane following it and ejected via the exhaust flap and via the interconnecting port to the second stage partially. As the inlet pressure drops the stage I exhaust flap closes and all the air passes to stage II, where it is further compressed and sent into the atmosphere. A gas ballast facility is available to enable the pump to pump the condensable gases without contaminating the oil. This is done by the introduction of gas at atmospheric pressure through a manually operated valve into the volume between the second stage rotor vane and discharge valve, when the mixture of air and the gases is at low pressure. When the volume of gas and vapor mixture is compressed prior to ejection, the discharge valve opens before the vapor can condense.

Oil diffusion pump

The oil diffusion pump consists of the following parts,

- The main body is cylindrical in shape which has a housing for the jet and the charging fluid. This is provided with a metallic flange. The pumps are fitted with a baffle valve to avoid backstreaming i.e., the migration of working fluid molecules into the system. A cooling water coil is soldered on the outer wall of the pump to cool the pump body.

- The jet consists of metallic nozzles which are assembled around a central rod and housed in the main body of the pump. All the nozzles are oriented downwards at a certain angle towards the water cooled pump body. The water circulated in the cooling coil cools the vapor down.

- The boiler is a part of the main body where the working fluid is heated and evaporated. The boiler is designed to hold a certain specified quantity of the recommended fluid. The boiler is heated electrically, with a heating element housed outside the main body. The heating element is properly secured to the main body by a suitable arrangement. The heating coil is well insulated from the main body and the heater cover. The terminals are provided on the other side of the heater cover to connect to the main power supply.

- The fore vacuum connection has a flange which is connected to the rotary vane pump. It is normally directed upwards and is cooled by water to avoid pump fluid being discharged to the atmosphere by the backing pump.

- Cold cap baffles are designed to in such a way that they can be mounted inside the pump body directly above

the top jet of the high vacuum stage. Cold-top jet baffles are used to reduce oil backstreaming. the cold cap has good thermal contact with the cooled wall of the pump which means it is practically at the cooling water temperature. A thermostat is fixed which acts as a safety device by cutting of the power supply to the heater when the cooling water does not work.

The oil in the boiler is heated by the heater and converted into vapor. this rises in the concentric columns and is limited by the jets due to the comparative high pressure existing above the boiler in the jet system. The vapor is forced through jet aperture where it is deflected downwards by jet deflectors while the tubular side jets discharge vapor into the backing system. The molecules issuing from the jet engulf gas molecules, diffuse into the vapor streams not being able to diffuse back due to the downward deflected vapors. The gas molecules are removed into the atmosphere by the backing pump. the oil vapor impinging on the water-cooled pump wall condenses and goes back into the boiler, where it is re-evaporated.

Vacuum Gauges

Mini Pirani Gauge can measure the pressure ranging from 0.5 mbar to 0.001 mbar.Two gauge heads are directly connected to this gauge to read the fore vacuum and the roughing vacuum of our vacuum system. A change of pressure in the vacuum system brings about a rise or fall in the number of gas molecules present and hence, a rise or fall in the thermal conductivity of the gas. The heat loss of the constant voltage electrically heated filament in the system varies with the pressure. The pirani gauge head filament has a high-temperature coefficient of resistance. So, a slight chanbe in the system pressure brings about a significant change in the filament resistance, resulting in an out-of-balance current, which can be read as the pressure in the meter. the Pirani gauge head indicates the total pressure of the gases and vapors. The mini Pirani gauge can also be used for leak detection through 'O' ring seals, door flanges, windows leak in shaft seals or valve diaphragm, hydrogen is ideally suitable as a probe gas in leak detection. Due to the high rate of diffusion through the leak, the Pirani gauge senses the change in pressure almost immediately. The thermal conductivity of Hydrogen gas is very high, which further enhances the gauge.

Mini Penning Gauge is designed with cold cathode-type gauge head. This gauge can be used to measure pressure ranges from 10^{-3}mbar to 10^{-6}mbar. This gauge is designed using the principle of emission of electrons from a cold cathode with a high voltage mode. The electrons emitted from the cathode of the gauge head are deflected by means of the magnetic field applied at right angles to the plane of the electrodes and are made to take the helical path before reaching the anode loop. This increases the probability of the electron colliding with the gas molecules. The secondary molecules produced by the ionization of the gas molecules themselves perform similar oscillations and the rate of ionization increases rapidly. Eventually, the electrons are captured by the anode and equilibrium is reached when the number of electrons produced per second by ionization is the sum of the positive ion current to the cathode and the electron current to the anode and is used to measure the pressure of the gas.

Electron Beam Vapour Deposition system

Electron beam evaporation, also known as E-beam, is a type of physical vapor deposition in which the target material to be used as a coating is exposed to an electron beam in order to evaporate and transform it into a gaseous state for deposition on the substrate. These atoms or molecules in a vapor phase precipitate and create a thin film coating on the substrate in a high vacuum chamber. It permits the direct transfer of energy with the Electron Beam to the target material to be evaporated, making it ideal for metals with high melting points. The electron beams are focused on the target material using magnetic coils. Since this system directly transfers the energy of the electrons to the target material, this system is suitable for materials with high melting points. he deposition rate can be controlled using quartz crystal rate sensors, temperature, or optical monitoring systems. he deposition rate can be controlled using quartz crystal rate sensors, temperature, or optical monitoring systems. This system requires high vacuum to deposit thin films on substrates. In our experiment, we used a scroll pump as a fore pump and a turbomolecular pump to get to the high vacuum range.

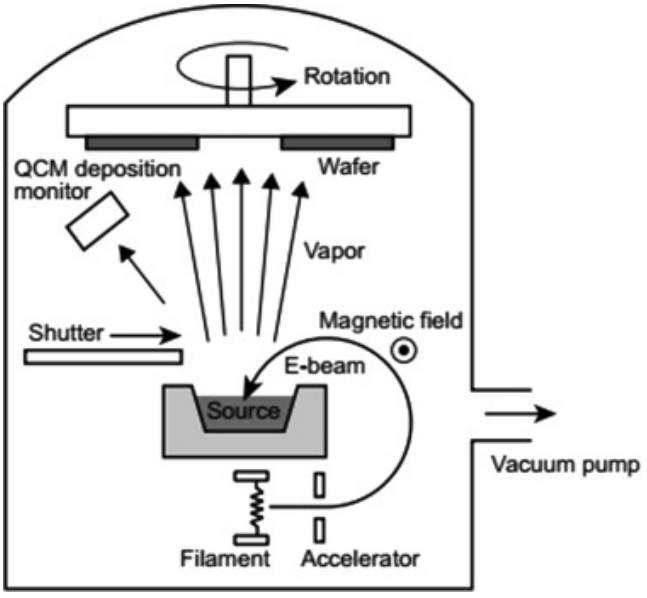

Figure 5: Schematic of electron beam deposition system

Scroll pump

Scroll pumps are dry vacuum pumps. Two co-wound spiral-shaped scrolls housed in a vacuum housing, with an exit valve in the middle, make up the basic functioning components of a scroll pump. While one spiral (the "orbiter") slides eccen-

trically against the other without rotating, the other spiral is fixed. As one of the spirals orbits, gas enters the (outside) open end of the spirals and is "squeezed and transported" between the two spirals, where it is caught between the scrolls and moved towards the centre. The volume that this limited "slug" of gas occupies reduces as it advances towards the centre, which causes it to be constantly compressed until it is released at pressure through a non-return valve at the housing's core. All of the moving elements in the chamber are self-lubricating, however the PTFE tip seals are prone to wear and will eventually need to be replaced.

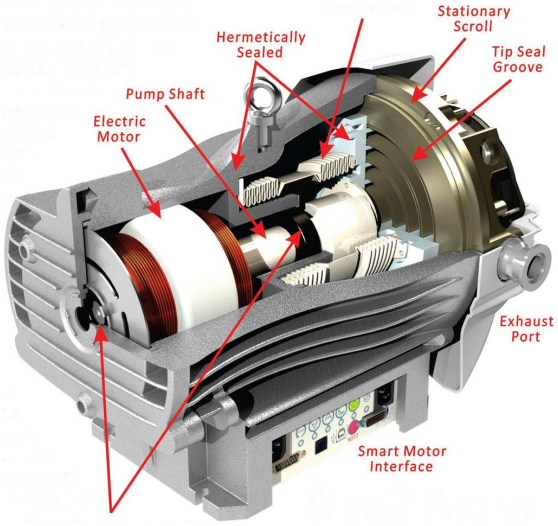

Figure 6: Scroll pump

Turbo-molecular pump

Turbomolecular pumps (TMPs) are kinetic vacuum pumps that operate using a very fast spinning rotor (usually rotating at between 24,000 and 90,000 RPM). Their typical operating pressures are in the high to ultra-high pressure range between 10-3 and 10-11 mbar. The pump works on the principle that gas molecules can be given energy by a quickly rotating rotor blade and stationary stator blade pair. Most turbomolecular pumps employ multiple stages, each consisting of a rotor blade and stator blade pair. The system is an axial compressor that puts energy into the gas, rather than a turbine, which takes energy out of a moving fluid to create rotary power. Gas captured by the upper stages is pushed into the lower stages and successively compressed to the level of the fore-vacuum (backing pump) pressure. The pumping speed remains constant over the entire working pressure range. It decreases at intake pressures above 10-3 mbar, as this threshold value marks the transition from the region of molecular flow to the region of laminar viscous flow of gases. The compression ratio of turbomolecular pumps is the ratio between the partial pressure of one gas component at the fore vacuum flange of the pump and that at the high vacuum flange. The pumping speed depends on the type of gas. The pumping effect of an arrangement consisting of rotor and stator blades is based upon the transfer of impulses from the rapidly rotating blades to the gas molecules being pumped. Molecules that collide with the blades are adsorbed there and leave the blades again after a certain period of time. In this process, blade speed is added to the thermal molecular speed. To ensure that the speed component transferred by the blades is not lost due to collisions with other molecules, the molecular flow must prevail in the pump, i.e., the mean free path must be greater than the blade spacing. The pumping speed of the pump can be compared with the catalog information.

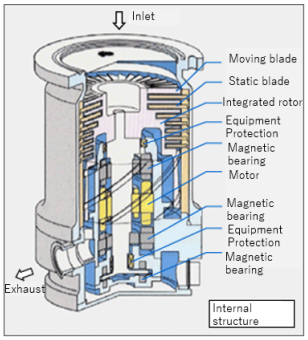

Figure 7: Turbomolecular pump

Thin film characterization

X-ray diffraction (XRD) and X-ray reflectivity (XRR) techniques were used in this experiment to study the film's crystal structure and thickness.

X-ray diffraction

X-ray diffraction is based on the interference pattern of monochromatic X-rays when they are incident on a thin film surface. A cathode ray tube produces the X-rays, which are then filtered to produce monochromatic radiation, focused by collimation, and pointed at the sample. When the circumstances are in accordance with Bragg's Law ($2dsin\theta = n\lambda$), the interaction of the incident rays with the sample results in constructive interference (and a diffracted ray). This law establishes a connection between the lattice spacing and diffraction angle in a crystalline sample and the wavelength of electromagnetic radiation. Then, these diffracted X-rays are identified, examined, and tallied. Due to the material's random orientation, all potential lattice diffraction directions should be obtained by scanning the sample through a range of 2 θ angles. Conversion of the diffraction peaks to d-spacings allows identification of the mineral because each mineral has a set of unique d-spacings. Typically, this is achieved by comparison of d-spacings with standard reference patterns.

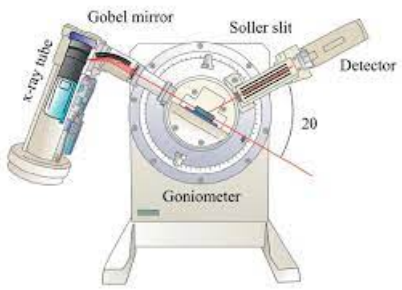

Figure 8: X-ray diffractometer

In a cathode ray tube, X-rays are produced by burning a filament to produce electrons, accelerating the electrons with a voltage towards a target, and then hitting the target material with the accelerated electrons. Characteristic X-ray spectra are created when electrons have enough energy to knock off the target material's inner shell electrons. The most prevalent k_α and K_β components in these spectra are among a number of others. K_α is made up in part of $K_{\alpha 1}$ and $K_{\alpha 2}$. $K_{\alpha 1}$ is twice as intense and has a slightly shorter wavelength than $K_{\alpha 2}$. Particular wavelengths characterize the target material (Cu, Fe, Mo, Cr). For the purpose of diffraction, monochromatic X-rays must be produced through filtering using foils or crystal monochrometers. The sample is exposed to collimated X-rays. The intensity of the reflected X-rays is measured while the sample and detector are rotated. A peak in intensity appears when the Bragg Equation is satisfied by the geometry of the incident X-rays impinging on the sample. This X-ray radiation is captured by a detector, which also processes it. The signal is then converted to a count rate and output to a printer or computer monitor, among other devices.

X-ray reflection

When electromagnetic waves are incident on a surface, a specularly reflected wave, a wave mad of diffused refractions, is generated. When X-rays are used, the refractive index of the material becomes less than 1 and we can observe total internal reflection below a certain grazing angle. An X-ray reflectivity curve observes a periodic oscillation in intensity related to the thickness of the thin film. The thickness of the thin layer can be found out by fourier transformation of the curve. The surface and the interface roughness can also be calculated using XRR data.

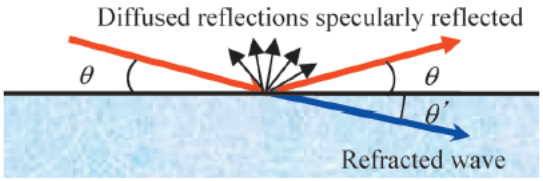

Figure 9: XRR schematic

Operation Procedure

The process of making thin films started with a silicon substrate. The substrate was first cleaned and then attached to the work holder of the electron beam vapor deposition system. Before loading the substrate, a scroll pump was used to create a low vacuum inside the chamber, after which the turbomolecular pump was used to create a high vacuum. A crucible filled with Nickel beads was placed below the work holder and an electron beam was focused on it. Nickel was used because it is paramagnetic and hence will be used for measuring transport properties. The thickness of the thin film was monitored using the quartz crystal sensor. After the deposition was complete, the thin films were taken for XRR and XRD characterization and the plots were analyzed.

Analysis

The XRD plot showed no peaks for Nickel, which suggested that the thin film formed was highly amorphous. The data from the XRR measurements (intensity vs. 2θ) were plotted in the Gen X software. The plots from the XRR characterization is shown below.

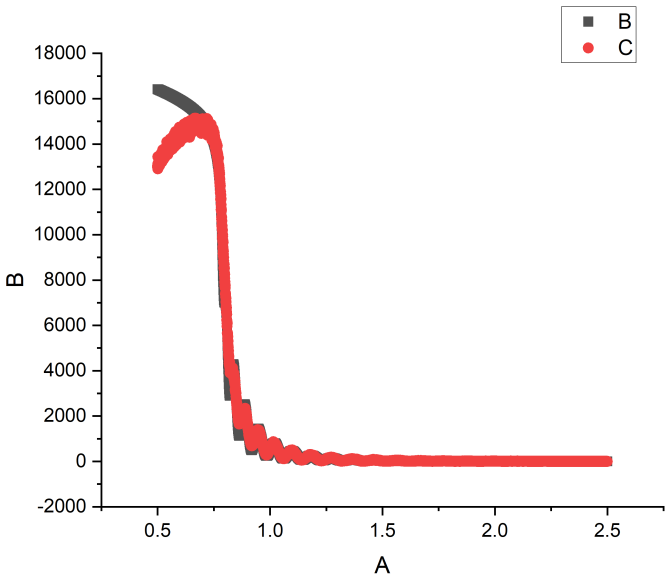

Figure 10: Data and the fitted plot from the XRR measurement of Nickel thin film. The red plot shows the observed plot, and the black plot shows the fitted plot.

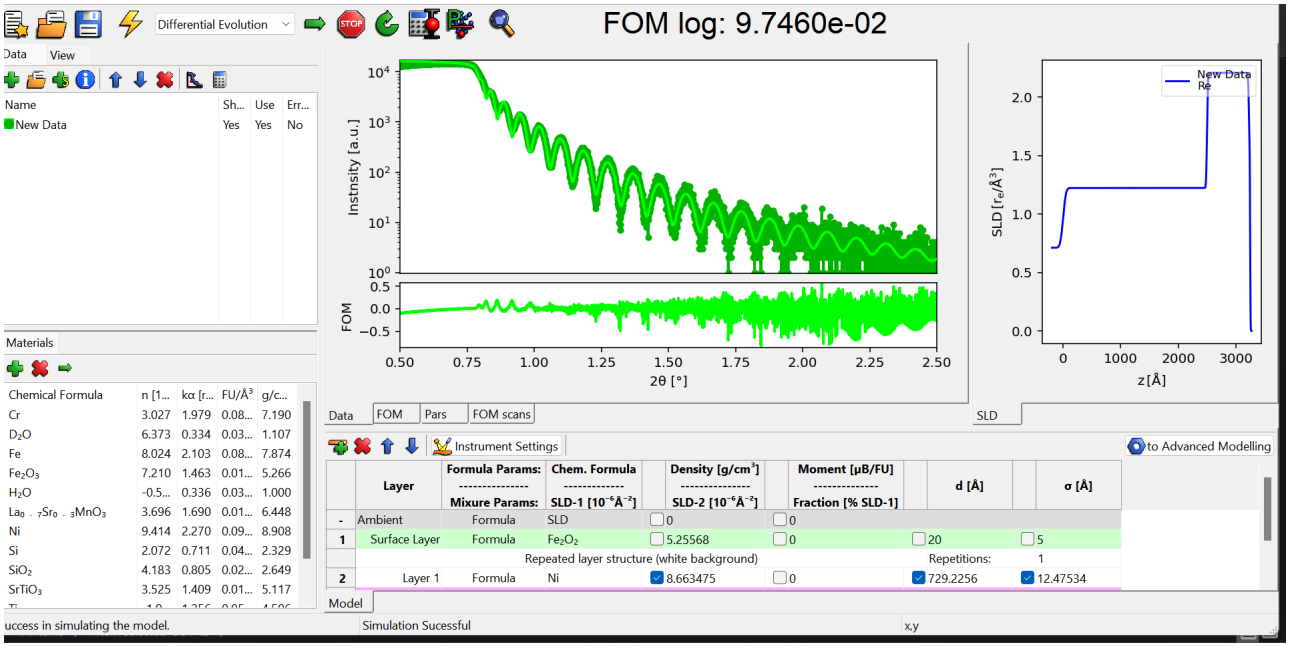

Figure 11: Screenshot of the fitting software Gen X 3.

The thickness of the thin film was found to be 729.22 Å, whereas the roughness was found to be 12.47 Å. The roughness is comparable to the thickness of the film, and hence, it suggests that the thin film is not deposited properly. However, transport properties can still be studied up to an extent using these films, which will be done in the following experiments.

The measurement probe

In order to measure the transport properties of the thin film, a probe was constructed. The design of the probe was inspired by the PPMS (Physical Properties Measurement System), although it was a highly downgraded version of the latter. The description of the probe is given below,

- The sample holder - The sample holder consists of a custom-cut PCB. The back of the PCB has a copper plate attached to it. A miniature heater and a silicon diode are attached to the back of the copper plate. The silicon diode is calibrated to measure the temperature. The calibration is done by providing a constant current across the silicon diode and measuring the potential difference across it at various known temperatures (for example, liquid nitrogen, ice water, frozen acetone, etc.). The relation between the temperature and the potential difference across the diode was linear for the temperature range in which we were working. All the components were attached to the PCB using Stycast - a two-part epoxy resin. This adhesive is thermally conducting and electrically insulating. Also, the coefficient of thermal expansion of Stycast is similar to that of copper. Hence it becomes a good choice for working at different temperatures. The posterior end of the PCB is cut so as to expose a square-shaped part of the copper plate to the front. This is where the sample has to be loaded. Copper wires are soldered to different columns of the PCB, and the other end of those wires go to the connection box (described later). To diode, the heater and the contact wires from the sample are all connected to the PCB via soldering.

- The shaft - The shaft is a hollow stainless steel tube, that holds together the sample holder and the connection box. Copper wires that are soldered to the PCB run inside the tube and go to the connection box.

- Connection box - The connection box is a stainless steel box with a removable lid. Ten banana females are fixed on one side of the box. The wires that are connected to the PCB are connected to the banana females. The stainless steel tube is fixed to an adjacent side of the connection box using Stycast and M-Seal. All the connections from voltage/current sources, voltmeters, etc. are given to this connection box.

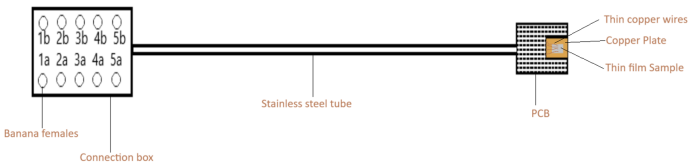

Figure 12: A schematic of the probe

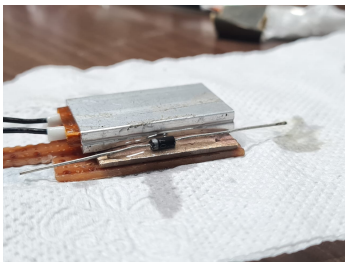

Figure 13: Rear part of the sample holder.

Measurement of resistivity of Nickel thin film.

To measure the resistivity of the sample, we used the four-probe method. The four-probe method requires four contacts arranged linearly on the sample. The outer two contacts provided current, and the inner two contacts were used to measure the voltage. The experimental setup is shown in the figure 14. The setup consists of a digital microvoltmeter, a constant current source, and the measurement probe with the sample. The two digital microvoltmeter was connected to sockets 2b and 3a using BNC to banana cable (refer figure 12). The constant current source was connected to sockets 2a and 3b. Voltage readings were taken for different values of current.

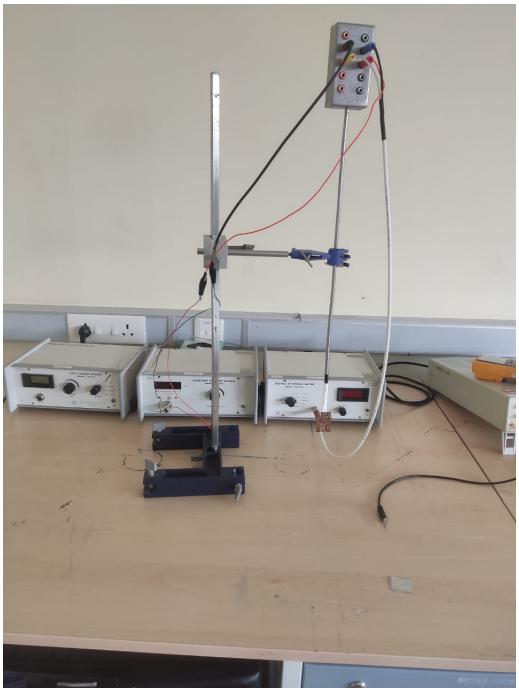

Figure 14: Experimental setup

The data and the plot of voltage vs. current are given below,

Current(mA)	Voltage(mV)
0.29	0.122
1.65	1.1
1.9	1.28
3.45	2.37
5.13	3.6
6.56	4.61
6.96	4.92
8.07	5.7
9.53	6.77
12.04	8.56
13.66	9.79
17.8	12.85
24.9	17.8
27.4	19.5
29.8	21.7
33.1	24.1
46.1	33.6
51.5	37.5
62.6	45.7
68.8	50.2
75.2	54.9
85.7	62.6
93.8	68.6
99.8	73
107.6	78.8
113.1	83.1
123.8	93.1
135.2	99.4
139.2	102.6
147.9	109.1
151.1	111.7
157	116.2
167.8	124.5
169.2	125.5
188.4	140.2

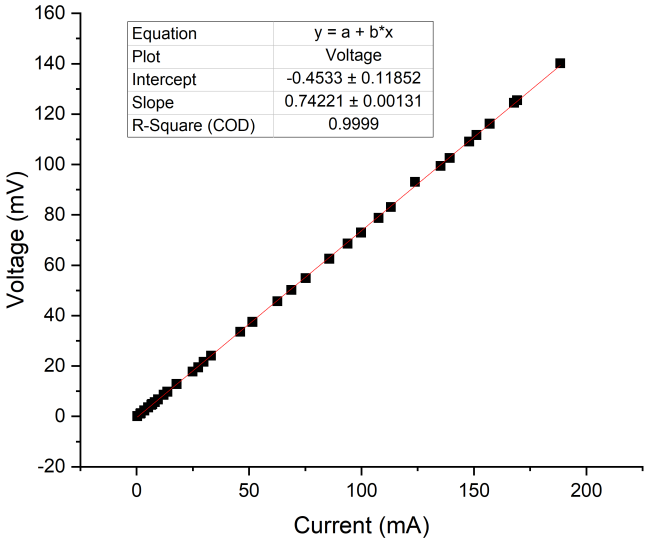

Figure 15: Plot of voltage vs current

From the plot, the slope is found to be 0.74221 Ω. The resistivity is then calculated as,

$$\begin{aligned} \rho &= \frac{\pi t}{ln(2)} \frac{V}{I} \\ &= 2.452 \times 10^{-7} \Omega m \end{aligned} \tag{1}$$

The error in resistivity is calculated as,

$$\begin{aligned} \frac{\delta\rho}{\rho} &= \frac{\delta m}{m} \\ &= 0.0018 \end{aligned} \tag{2}$$

$$\delta\rho = 0.0044 \times 10^{-7} \Omega m$$

Results and Conclusion

The resistive thermal vapor deposition system is one of the cheapest and most efficient deposition systems. The electron beam deposition system requires a higher vacuum to work and is much more complex than the resistive thermal vapor deposition system. However, the quality of thin films is better. This experiment was a good opportunity to learn about the resistive thermal vapor deposition system. The thin films that are created will be used to measure the hall coefficient and magnetoresistance of nickel and show the correlation of both quantities with temperature.

The resistivity of nickel thin film is found to be $(2.452 \pm 0.0044) \times 10^{-7} \Omega m$. The resistivity was found using the four-probe method. The literature value of the resistivity of nickel at 20^oC is $7 \times 10^{-8} \Omega m$. The deviation of our observed value from the literature value is more than one order of magnitude. This deviation can be attributed to certain possible sources of error.

- The contacts on our sample were not properly made. The area of contact might not have been sufficiently small. Since they kept breaking from time to time, the contacts had to be made repeatedly.
- The sample was prepared a long time before it was used for measurement, hence there might be a possibility of contamination.
- The contacts in the four-probe method were not linear, as they should be.

Other than these sources of error, there might have been other sources that might have been missed. Although the experiment could not give us the desired results, it provided a great insight into vacuum technology and thin film techniques. The measurement probe designed in this experiment can also be used to measure other transport properties like magnetoresistance, and hall effect for different samples.

1 References

- https://www.semicore.com/news/89-what-is-e-beam-evaporation
- https://sens4.com/pirani-working-principle.html
- http://lampes-et-tubes.info/vg/vg036.php?l=e
- https://showcase.ulvac.co.jp/en/how-to/product-knowledge02/turbo-molecular-pump.html
- Handbook of thin film deposition processes and techniques, 2nd ed., Krishna Seshan
- Stephen Ogbonna Mbam et al 2019 Mater. Res. Express 6 122001
- Thin films: Preparation, charactrerization, Applications, Manuel P. Soriaga *et. al*